SnT 2023
CTBT: SCIENCE AND TECHNOLOGY CONFERENCE
HOFBURG PALACE - Vienna and Online
19 TO 23 JUNE

A New Method of Seismometer Orientation Correction via Amplitude and Energy Based Teleseismic Receiver Function Measurements: Test Case on West Africa and Adjacent Islands

Abayomi Gaius OSOTUYI[1], Sidao NI[1,2], Jiajun CHONG[2]
1.University of Science and Technology of China
2. Academy for Precision Measurement Science and Technology, CAS, China

INTRODUCTION

We seek to establish a robust method of determining and correcting the misorientation seismic stations with radial and tangential components of teleseismic receiver function (RFs)

METHODS/DATA

Using the amplitude method (PRFamp) and energy (PRFenergy) of P-wave receiver function (PRFs) using varying Gaussian factors with equivalent cutoff frequencies. We estimate the misorientation of 26 permanent seismic stations across West Africa and its adjacent Islands

START

RESULTS

Tests to examine the effect of varying Gaussian factors on the estimates of misorientation are more noticeable in results from stations for which RFs are indicative of 3D or complex structures and islandic stations. Results from both methods show good correlation.

CONCLUSION

PRFamp method proves to be more stable due to their proximity to the statistical mean and standard deviation results. Gaussian factor of 1.5 1.5 is recommended as a trade-off. We suggest that multiple approaches be adopted to provide robust bases for the misorientation estimation

Please do not use this space, a QR code will be automatically overlayed

P4.2-083

INTRODUCTION

- Accurate seismic station orientation is essential for seismic waveform data quality and seismo-logical studies

- In modern seismological observation networks, seismic events are recorded by orthogonally aligned triaxial sensors. Although the assumption holds that single vertical-component sensors do not have misorientation concerns, the two horizontal components involving the BHN (north–south) and BHE (east–west) may have misorientation issues (Niu and Li, 2011; Wang et al., 2016; Doran and Laske, 2017; Ekström and Nettles, 2018; Langston, 2018; Ojo et al. 2019; Zheng et al. 2020)

- Previously, misorientation errors have been estimated using tangential components from P-wave energy minimization, P-wave particle motion, and Rayleigh-wave angle of arrival measurements (Doran and Laske, 2017; Ekström and Nettles, 2018; Langston, 2018; Ojo et al. 2019; Zheng et al. 2020)

- In this study, we conduct a series of tests involving different α values to investigate the amplitude-based (hereafter referred to as PRFamp) method using the single-point maximum amplitude of RF and energy-based (hereafter referred to as PRFenergy) method that utilize a time window around the maximum amplitude of the P-wave receiver function (PRFs).

- We used 26 permanent stations cutting across the Inland, Coastal, and Islandic terrains of West Africa to test our methods.

INTRODUCTION
OBJECTIVES
METHODS/DATA
RESULTS
CONCLUSION

Please do not use this space, a QR code will be automatically overlayed

METHOD

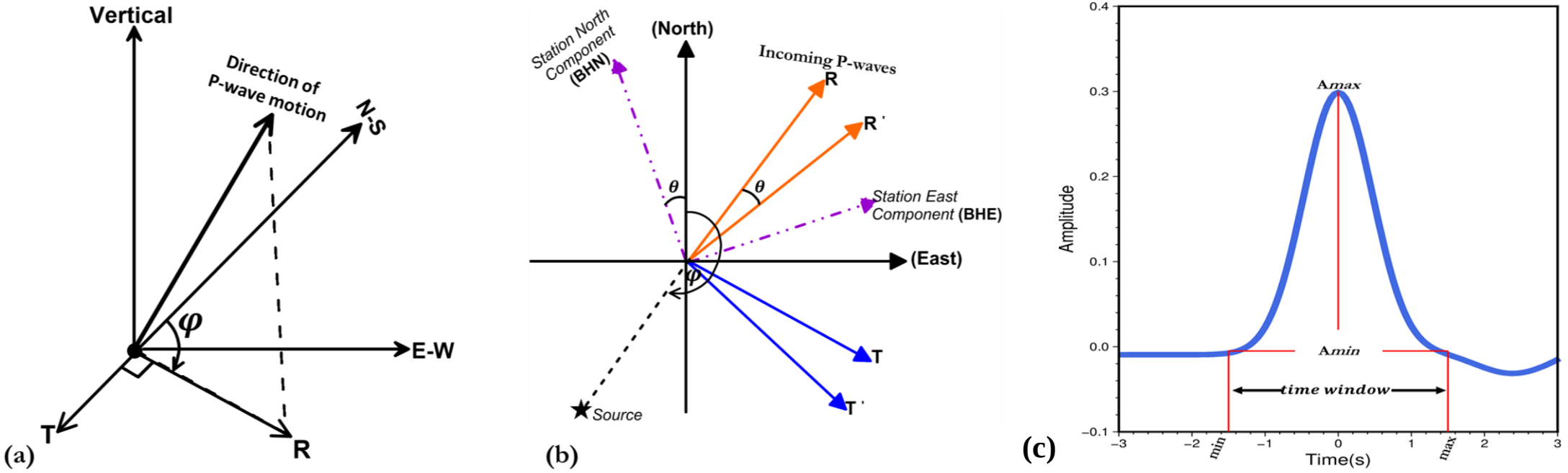

- (a) Coordinate geometry of seismic station relative to the direction of P-wave motion from the source.
- (b) Station components and direction of horizontal components of the P-wave window. R and T are radial and tangential components relative to the seismometer's orientation. R′ and T′ are radial and tangential components after orientation correction with the angle "Theta" (θ).
- (c) The amplitude and time window in the vicinity of 0 seconds of P-phase of the *RRC*. The minimum and maximum values for both time and amplitudes vary for different Gaussian factors (*α* values are (0.5, 1.0, 1.5, 2.5, 3.0, and 5.0)

INTRODUCTION
OBJECTIVES
METHODS/DATA
RESULTS
CONCLUSION

Please do not use this space, a QR code will be automatically overlayed

METHOD – Study location and Data

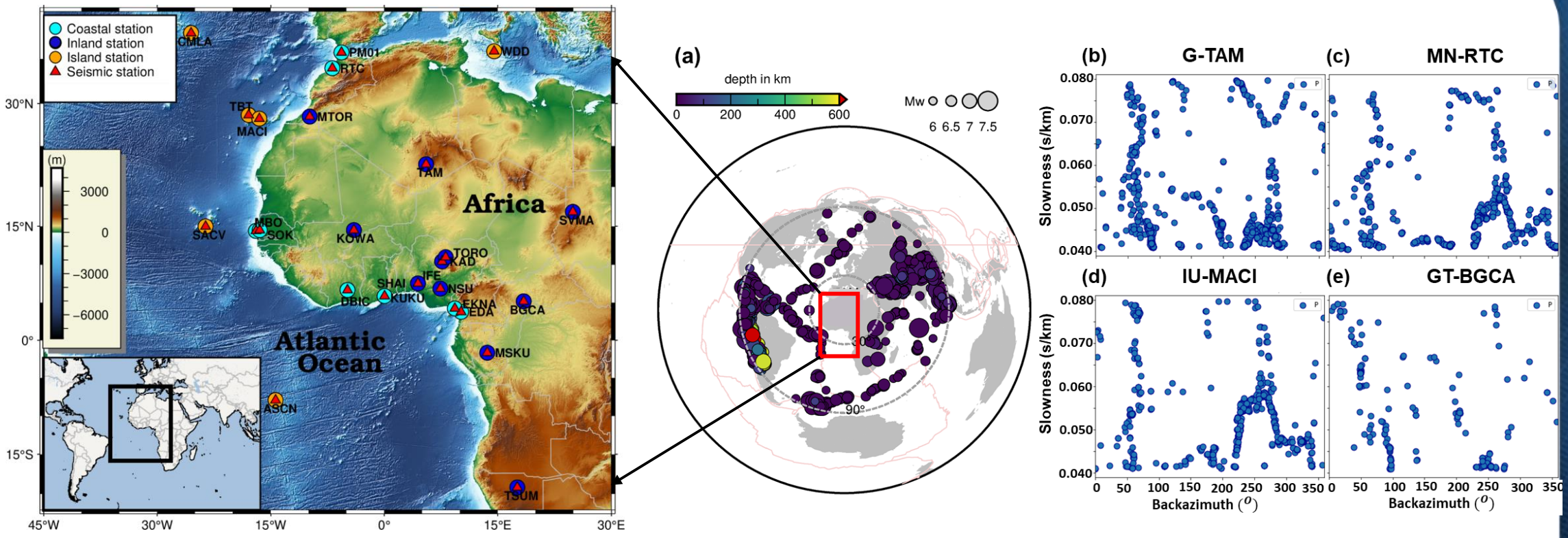

- (a) The study area showing seismic recording stations and equidistant-azimuthal distribution of teleseismic earthquakes around the study area; January 1990 to March 2021.
- (b–e) The distribution of P-wave RFs event slowness against the back-azimuthal distribution

INTRODUCTION
OBJECTIVES
METHODS/DATA
RESULTS
CONCLUSION

Please do not use this space, a QR code will be automatically overlayed

RESULTS – Receiver function

i

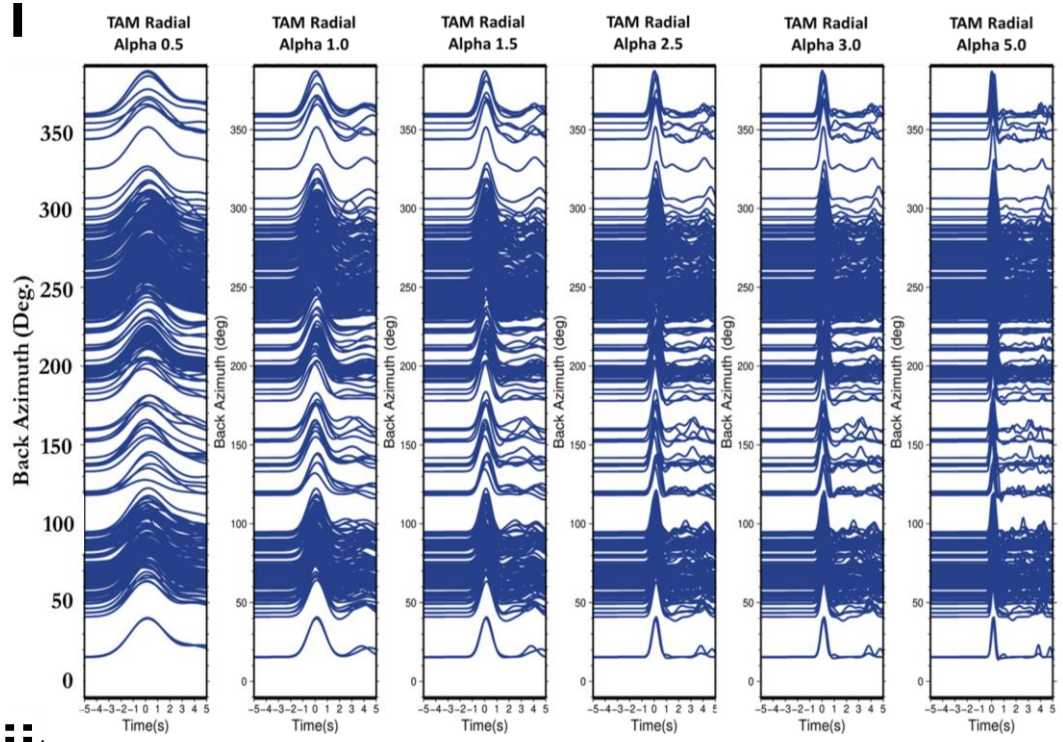

ii

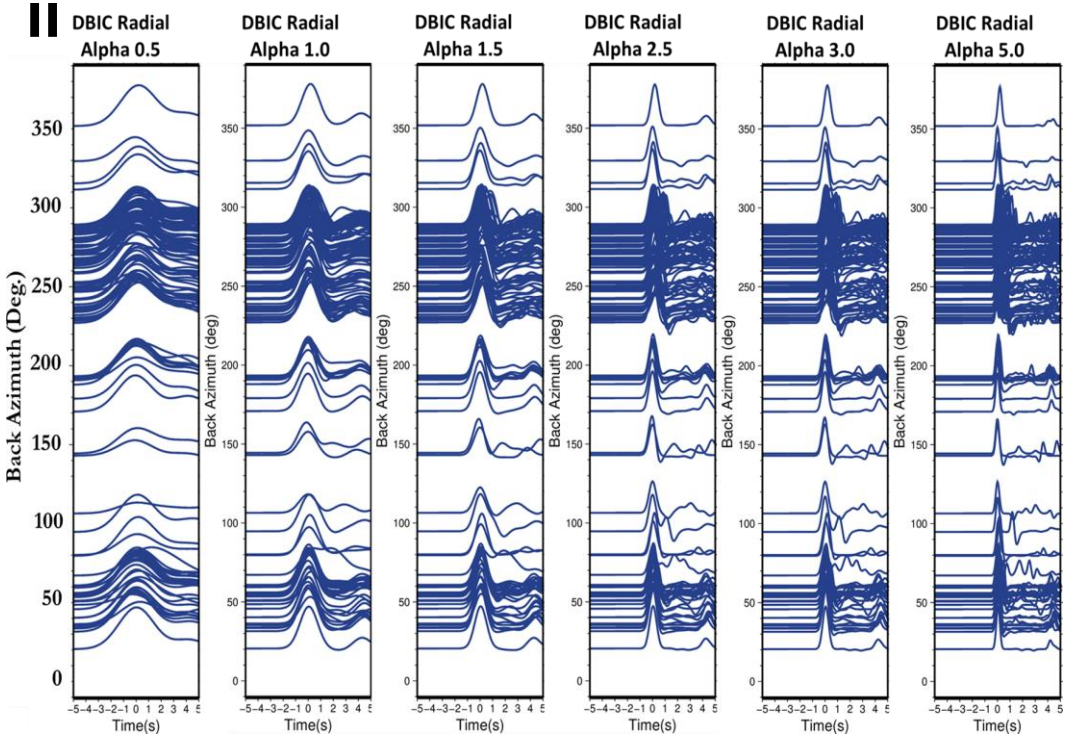

iii

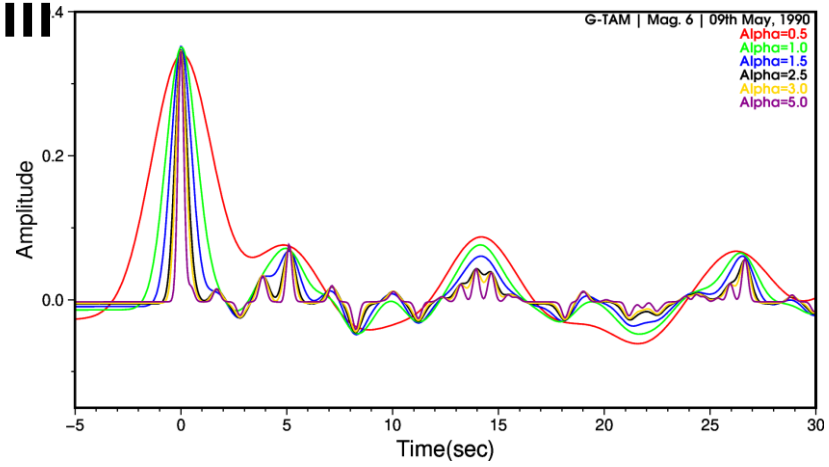

- RFs were computed in the frequency domain

Osotuyi et al., 2023 *SRL*

- RFs are windowed between −5 and 5 s
- (i) PRF at representative stations G-TAM and (ii) GE-DBIC showing results for different α
- (iii) Effect of varying α on RFs

INTRODUCTION
OBJECTIVES
METHODS/DATA
RESULTS
CONCLUSION

Please do not use this space, a QR code will be automatically overlayed

RESULTS – Search for the best orientation

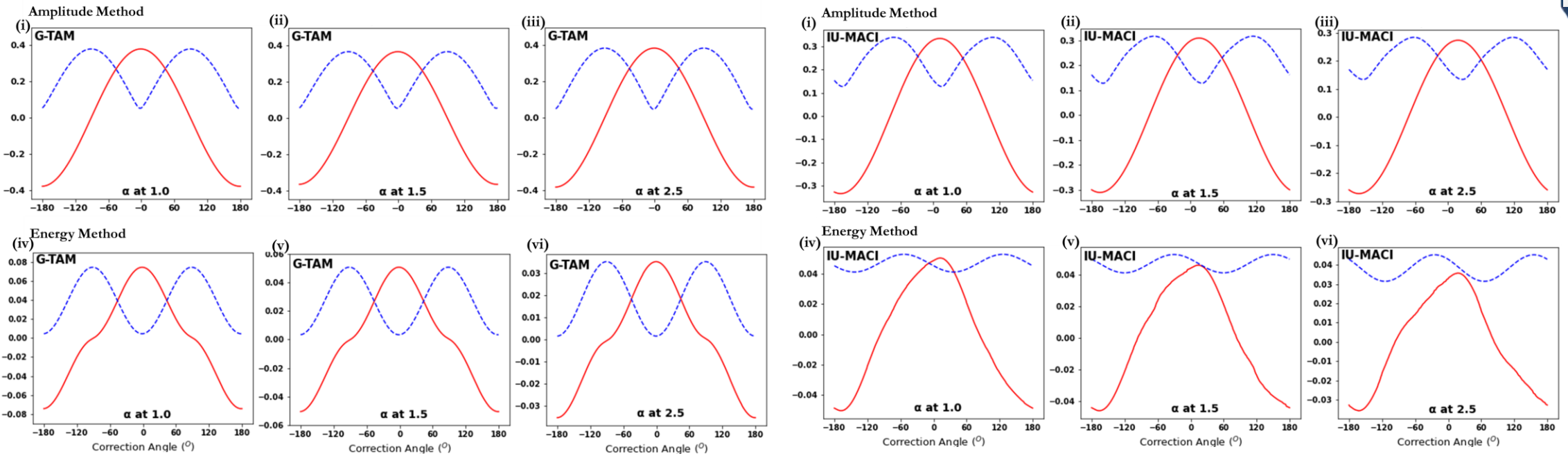

Osotuyi et al., 2023 *SRL*

- The red and blue lines in the plots correspond to objective functions from RRC and RTC
- Consideration of the objective functions involving maximum amplitude of RRC, minimum of RTC, and the energy of the RRC
- The IU-MACI station is an island station for which RFs reveal complex subsurface heterogeneities underlying the station

INTRODUCTION
OBJECTIVES
METHODS/DATA
RESULTS
CONCLUSION

Please do not use this space, a QR code will be automatically overlayed

RESULTS – Misorientation variation with Time and Backazimuth

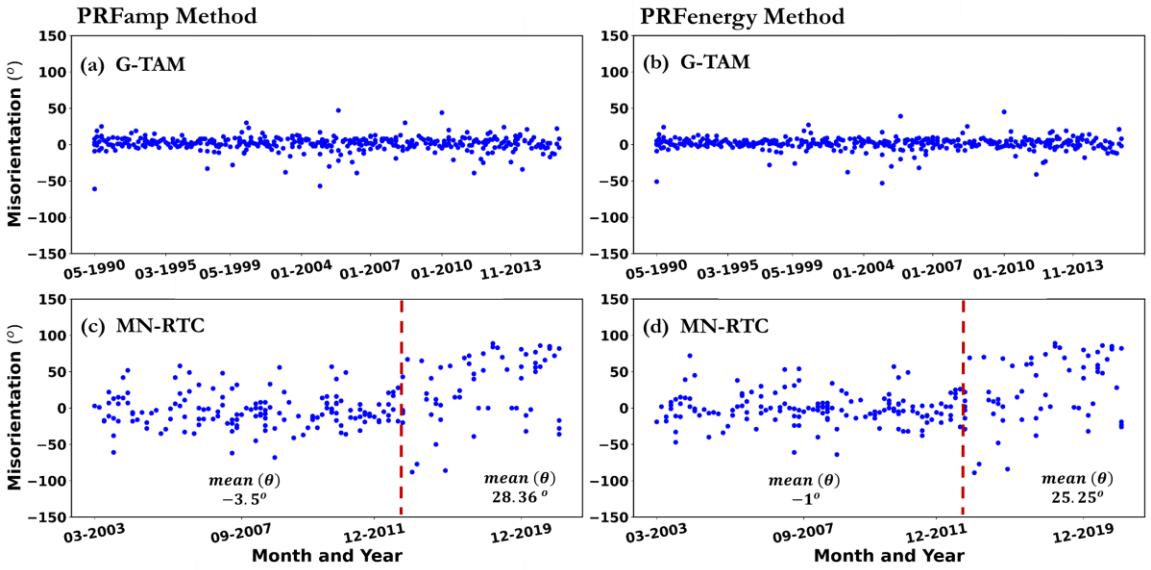

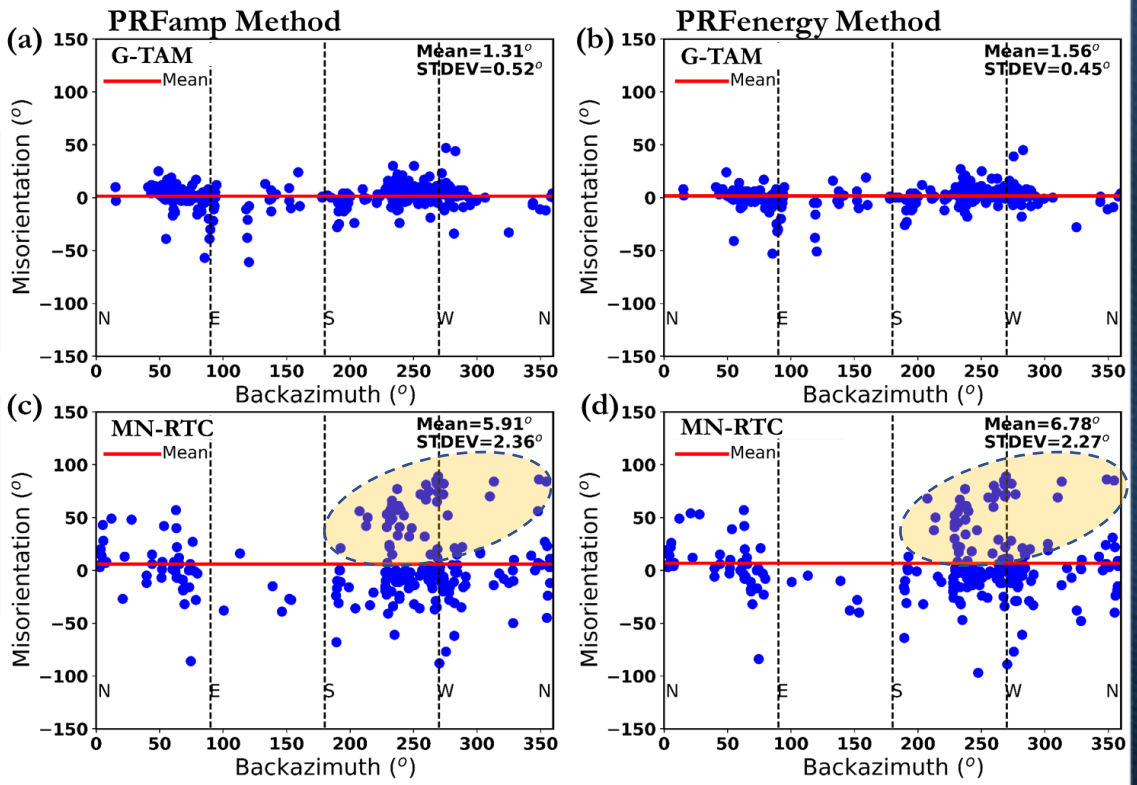

- Sensor orientation variation with time (black) and sensor orientation variation with back azimuth through the validation periods at the representative

- Back-azimuthal distribution with sensor misorientation variation through the validation periods at the representative

INTRODUCTION
OBJECTIVES
METHODS/DATA
RESULTS
CONCLUSION

Please do not use this space, a QR code will be automatically overlayed

RESULTS – Statistical Analysis

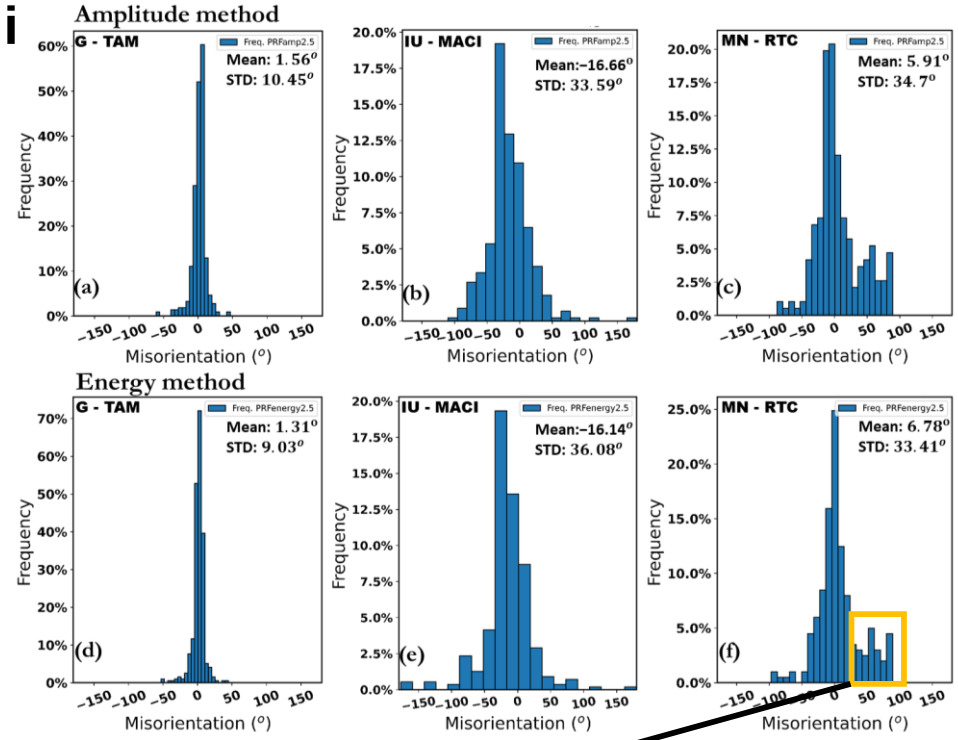

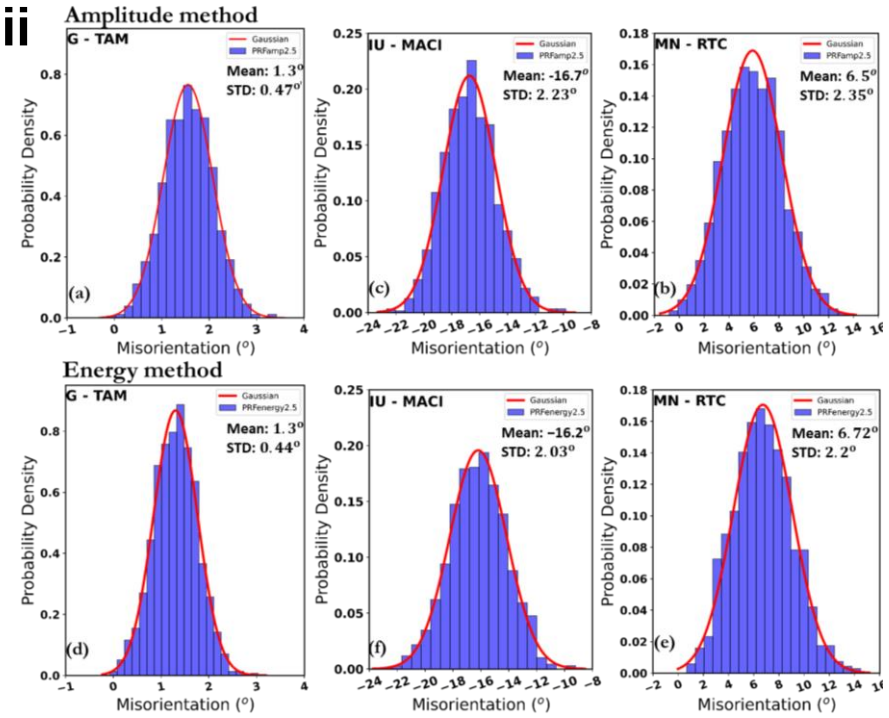

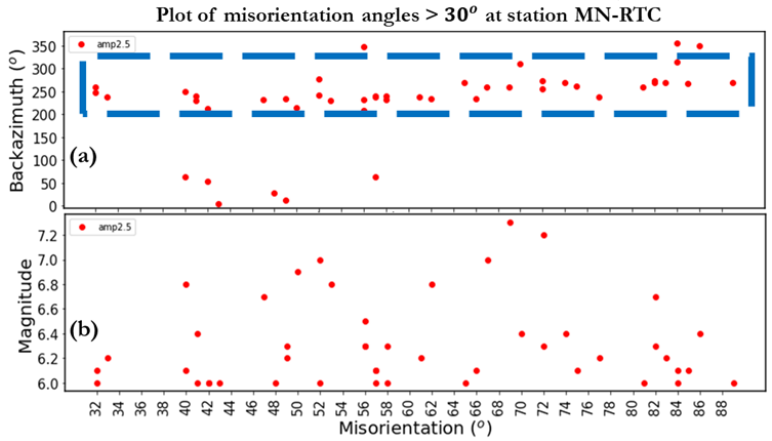

- i(a–f) Frequency and ii(a-f) probability distribution of sensor misorientation estimates from events at representative stations G-TAM, IU-MACI, and MN-RTC
- Misorientation angles > 30° in i(a–f) against (a) Backazimuth and (b) Magnitude in station MN-RTC showing non-Gaussian distribution on the graph

INTRODUCTION
OBJECTIVES
METHODS/DATA
RESULTS
CONCLUSION

Please do not use this space, a QR code will be automatically overlayed

RESULTS –
Correlation of both methods and effect of number of events

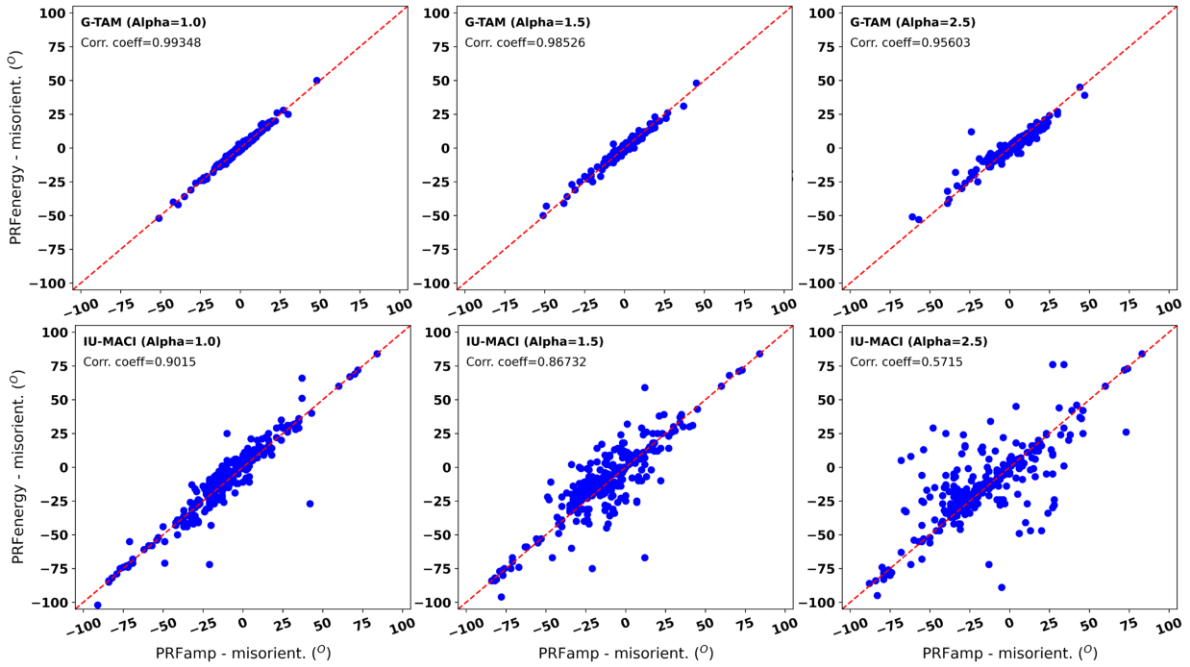

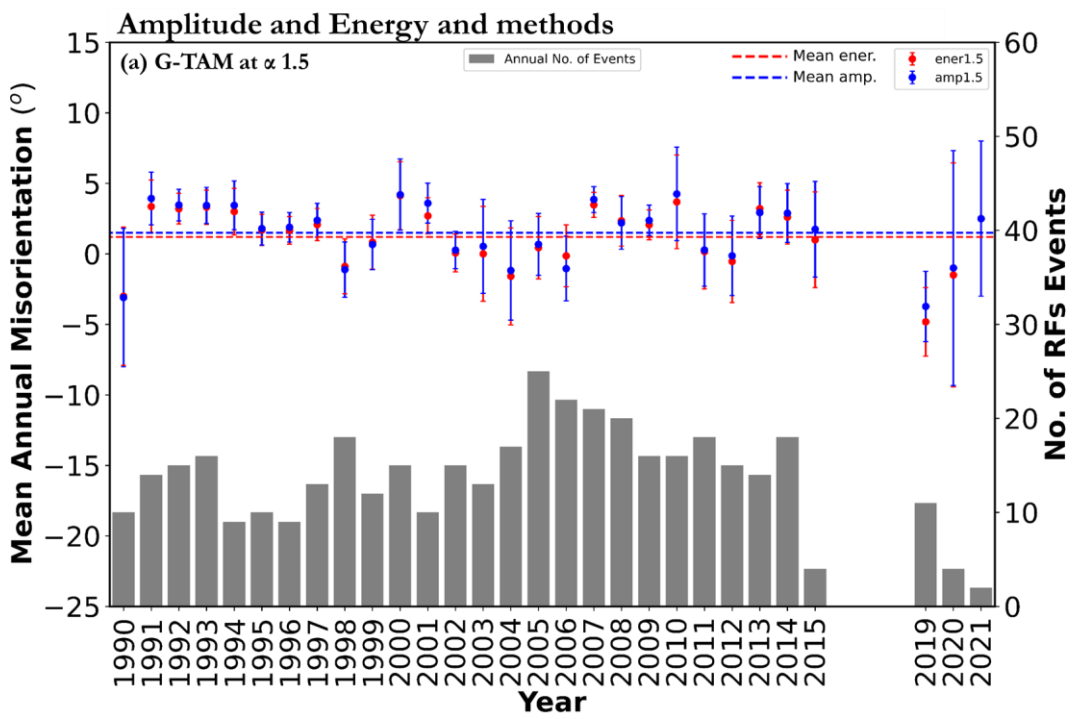

- PRFamp vs PRFenergy of varying α, and correlation coefficient
- Relationship between yearly recorded RFs, annual mean misorientation estimates, and annual error estimation of recorded events at station G-TAM

INTRODUCTION
OBJECTIVES
METHODS/DATA
RESULTS
CONCLUSION

Please do not use this space, a QR code will be automatically overlayed

RESULTS –
Station distribution and effect of misorientation

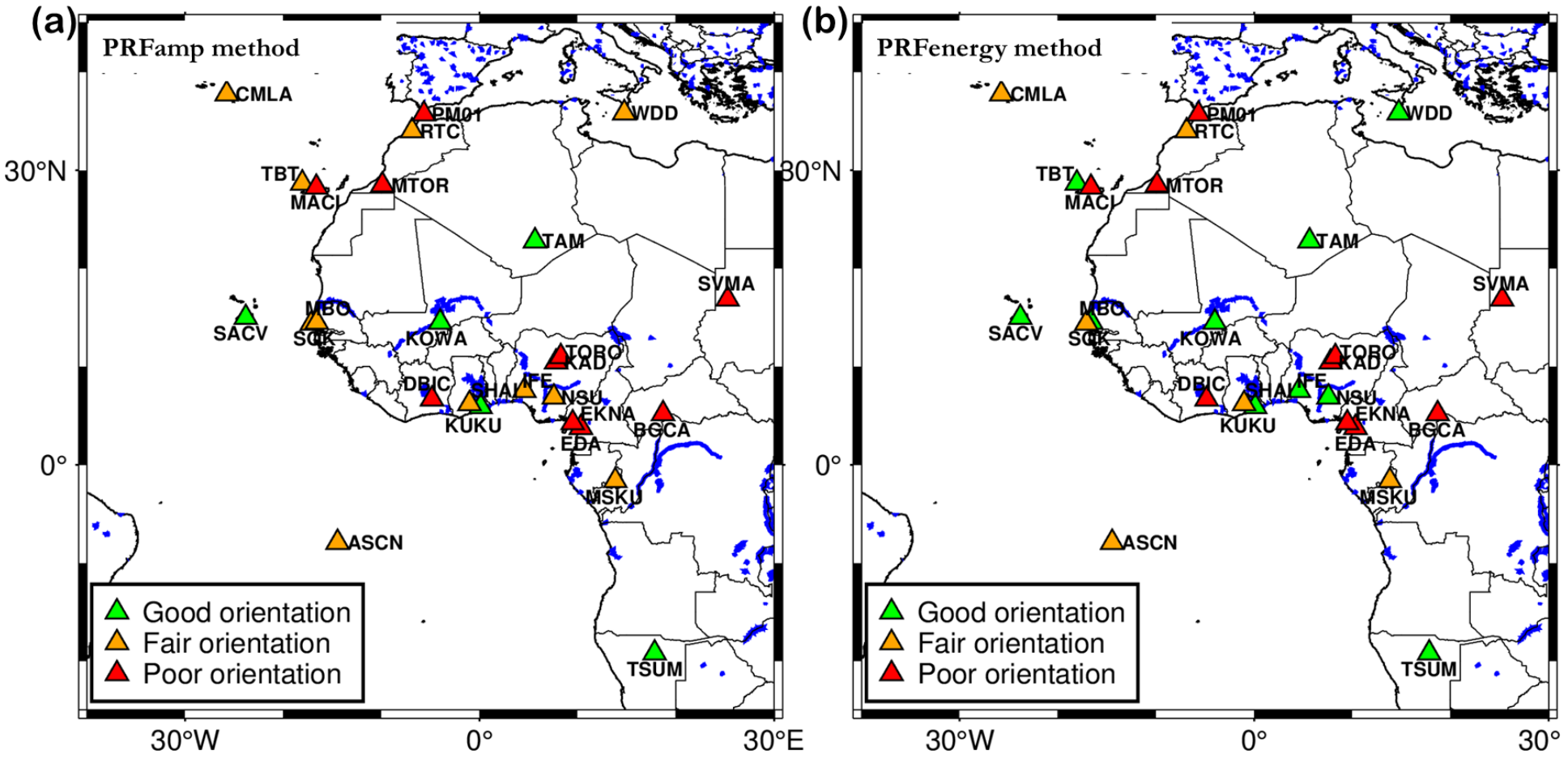

Osotuyi et al., 2023 *SRL*

- **Corresponding estimated sensor misorientation correction for PRFamp and PRFenergy methods across different terrains**

INTRODUCTION
OBJECTIVES
METHODS/DATA
RESULTS
CONCLUSION

Please do not use this space, a QR code will be automatically overlayed

RESULTS-
Effect of orientation correction on RFs and RFHV Waveforms

i

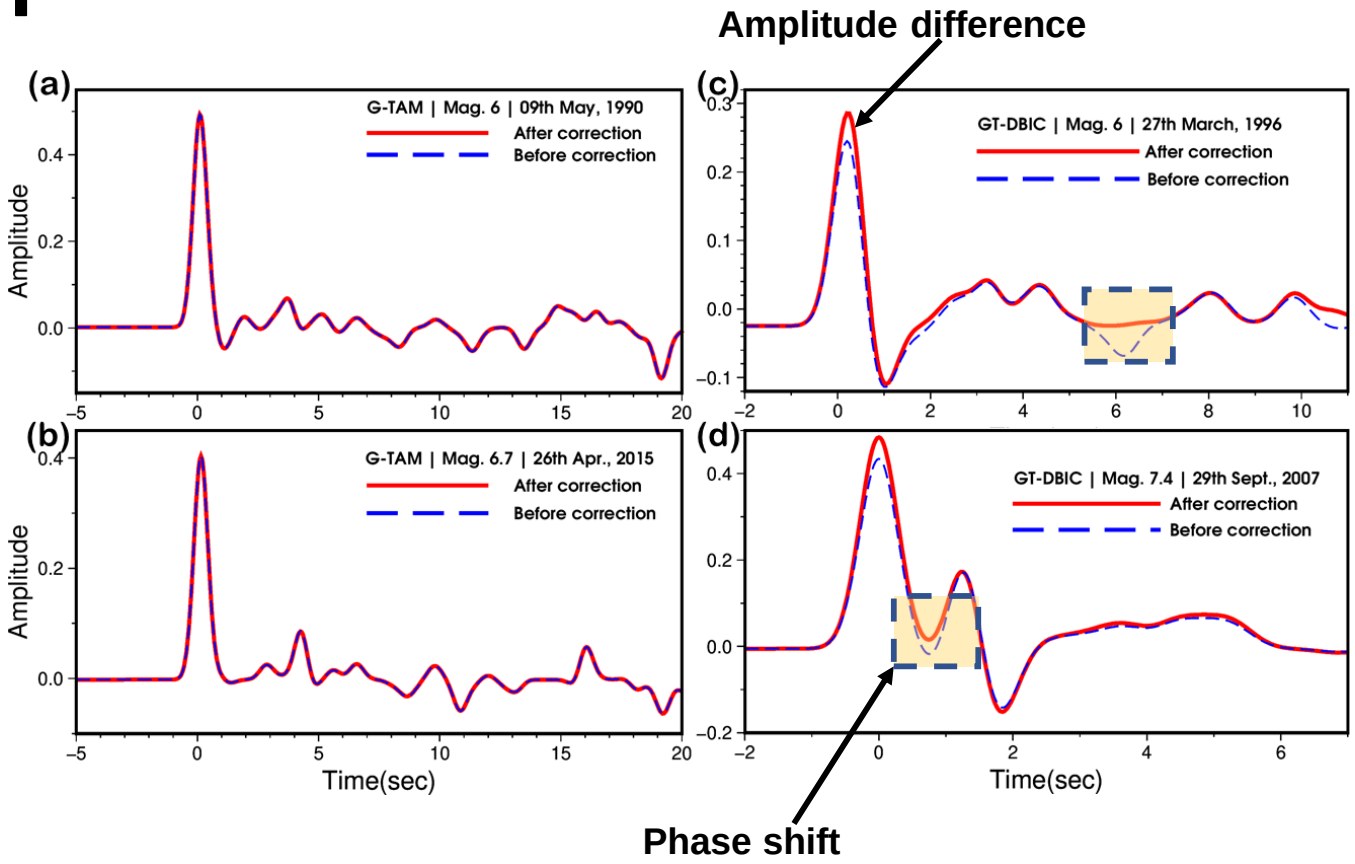

ii

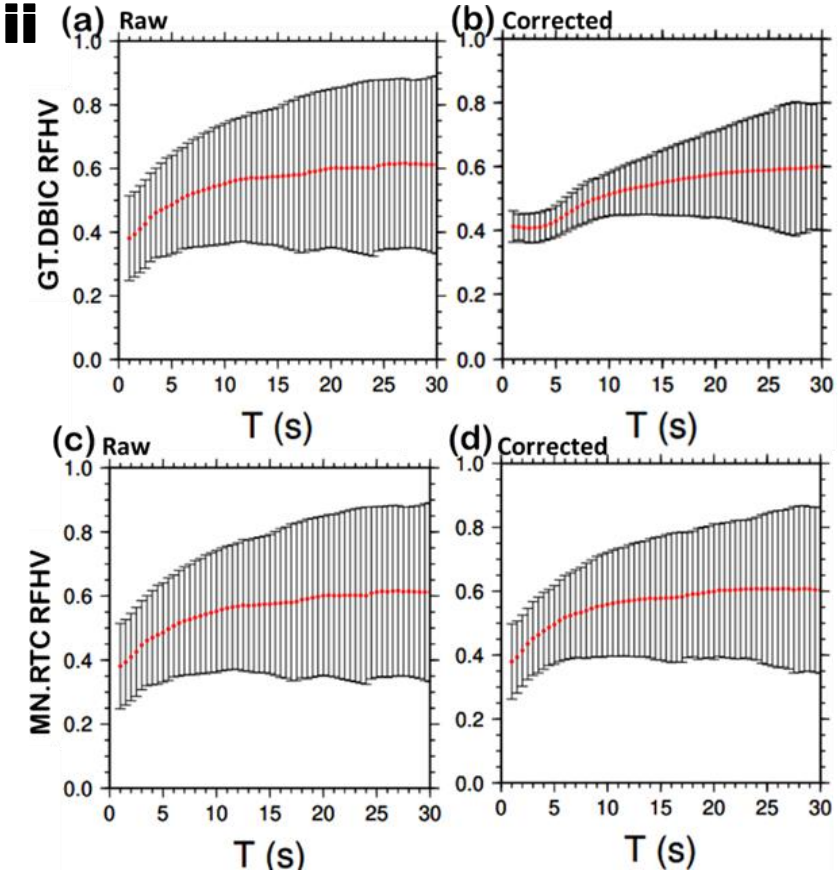

In progress

- i(a – d) Effect of misorientation correction on RFs at stations G-TAM (Good) and GT-DBIC (Poor)
- ii(a – d) Effect of misorientation correction on RFHV ratio results at GT-DBIC and MN-RTC

INTRODUCTION
OBJECTIVES
METHODS/DATA
RESULTS
CONCLUSION

Please do not use this space, a QR code will be automatically overlayed

RESULTS – Comparison of results with previous study

S/No.	Network	Station	No. of Events	PRFamp method (angles are in degrees)				PRFenergy method (angles are in degrees)			Difference in PRFamp and PRFenergy methods (Δα)			Ojo et al., 2019		
				α=1.0	α=1.5	α=2.5		α=1.0	α=1.5	α=2.5	Δα=1.0	Δα=1.5	Δα=2.5	M1-BHN	M2-BHN	M3-BHN
1	G	TAM	402	1	1	1		1	1	0	0	0	1	1.8	1.96	2.15
2	IU	TBT	55	-8	-10	-11		-1	-0.4	-8	7	9.6	3	-7.2	-5.46	-3.21
3	IU	MACI	310	-12	-14	-17		-10	-12	-16	2	2	5	-7	-7.98	-8.17
4	G	MBO	315	-6	-6	-7		-5	-5	-6	1	1	2	-8.7	-9.59	2.05
5	GT	DBIC	138	17	17	17		17	17	18	0	0	1	14.9	14.14	15.43
6	AF	IFE	32	25	25	30		25	25	29	0	0	1	-21.7	-17.79	176.71
7	AF	KUKU	80	7	7	7		7	6	6	0	1	1	4.4	3	-0.12
8	MN	RTC	216	6	6	5		6	7	7	0	1	2	-5.8	-2.37	-8.15
9	GT	BGCA	135	11	11	11		11	11	11	0	0	0	10.9	10.78	10.76
10	IU	MSKU	48	5	5	12		5	5	12	0	0	0	5.6	8.48	19.62
11	II	ASCN	58	-6	-7	-5		-5	-9	-9	1	2	4	-0.7	-1.28	-2.37
12	MN	WDD	662	4	4	5		3	3	3	1	1	2	-4	-3.92	-1.84
13	IU	TSUM	357	3	2	2		3	2	4	0	0	2	6.6	7.15	-4.26

Classification

$0 - \leq 3^o = Good$

$4^o - \leq 10^o = Fair$

$> 10^o = Poor$

INTRODUCTION
OBJECTIVES
METHODS/DATA
RESULTS
CONCLUSION

Please do not use this space, a QR code will be automatically overlayed

CONCLUSION

- Misorientation correction shows significant effect on RFs waveforms and RFHV analysis
- The effect of heterogeneity was insignificant on PRFamp in comparison with PRFenergy method i.e. the latter is more sensitive to subsurface heterogeneities and/or dipping interfaces
- station misorientation errors or accuracy may not be influenced by or dependent on the back-azimuthal distribution of events
- In all the stations but one, the stations showed a relatively stable range of misorientation values during the recording period
- the number of events used for misorientation estimation could significantly impact the results. A minimum of 30 events are recommend for station orientation analysis
- Results from an α of 1.5 are recommended as a trade-off between oversimplification and complications due to subsurface structures
- Physical interaction with sensors should be limited. Transmission (telemetry) of waveforms is recommended

INTRODUCTION
OBJECTIVES
METHODS/DATA
RESULTS
CONCLUSION

Please do not use this space, a QR code will be automatically overlayed

REFERENCES

- Burdick, L. J., and C. A. Langston (1977). Modeling crustal structure through the use of converted phases in teleseismic body-wave forms, Bull. Seismol. Soc. Am. 67, 677–691
- Chong, J., R. Chu, S. Ni, Q. Meng, and A. Guo (2018). Receiver function HV ratio: A new measurement for reducing non-uniqueness of receiver function waveform inversion, Geophys. J. Int. 212, 1475–1485
- Doran, A. K., and G. Laske (2017). Ocean-bottom seismometer instrument orientations via automated Rayleigh-wave arrival-angle measurements, Bull. Seismol. Soc. Am. 107, no. 2, 691–708, doi: 10.1785/0120160165
- Efron, B. (1979). Bootstrap methods: Another look at the jackknife, Ann. Stat. 7, no. 1, 1–26.
- Ekström, G., and M. Nettles (2018). Observations of seismometer calibration and orientation at USArray Stations, 2006–2015, Bull. Seismol. Soc. Am. 108, no. 4, 2008–2021, doi: 10.1785/0120170380
- Langston, C. A. (2018). Calibrating dense spatial arrays for amplitude statics and orientation errors, J. Geophys. Res. 123, 3849–387
- Laske, G. (1995). Global observation of off-great-circle propagation of long-period surface waves, Geophys. J. Int. 123, no. 1, 245–259
- Lim, H., Y. Kim, T. A. Song, and X. Shen (2018). Measurement of seismometer orientation using the tangential P-wave receiver function based on harmonic decomposition, Geophys. J. Int. 212, 1747–1765
- Niu, F., and J. Li (2011). Component azimuths of the CEArray stations estimated from P-wave particle motion, Earthq. Sci. 24, 3–13
- Ojo, A. O., S. Ni, and Z. Li (2017). Crustal radial anisotropy beneath Cameroon from ambient noise tomography, Tectonophysics 696/ 697, 37–51, doi: 10.1016/j.tecto.2016.12.018
- Ojo, O. A., L. Zhao, and X. Wang (2019). Estimations of sensor misorientation for broadband seismic stations in and around Africa, Seismol. Res. Lett. 90, no. 6, 2188–2204, doi: 10.1785/0220190103
- Oni, A. G., Eniola, J. P., Olorunfemi, M. O., Okunubi, M. O., Osotuyi, A. G. (2020). The magnetic method as a tool in groundwater investigation in a basement complex terrain: Modomo Southwest Nigeria as a case study. Springer - Applied Water Science. https://doi.org/10.1007/s13201-020-01279-z
- Osotuyi, A. G., Mohammed, M. Z., Ajayi, I. R., Salako A. O. (2021). Assessment of Geoelectric Properties and Localized Geology as Indicators on Cocoa (Theobroma Cacao) Yield in Part of Southwestern Nigeria. Elsevier- Heliyon. https://doi.org/10.1016/j.heliyon.2021.e08516
- Osotuyi, A. G., S. Ni, J. Chong, X. Jun, and O. Akpan (2023). Seismometer orientation correction via Teleseismic Receiver Function measurements in West Africa and adjacent Islands – Accepted Seismological Research Letters. Doi: 10.1785/0220220316.
- Osotuyi, A., A. Falade, A. Adepelumi, and S. Onibiyo (2022). Thermal anomaly and land surface temperature associated with the Abuja, Nigeria earth Tremor of 7th September 2018, Springer Advances in Science, Technology & Innovation, doi: 10.1007/978-3-030-73026- 0_54
- Salako, A. O., A. G. Osotuyi, and A. A. Adepelumi (2019). Seepage investigations of heterogeneous soils beneath some buildings using geophysical approaches: Example from southwestern Nigeria, Int. J. Geo-Eng. 10, doi: 10.1186/s40703-019-0107-5
- Song, Z., X. Zeng, B. Chi, F. Bao, and A. G. Osotuyi (2022). Using the three station interferometry method to improve urban DAS ambi ent noise tomography, Front. Earth Sci. 10, doi: 10.3389/feart.2022.952410
- Wang, X., Q. F. Chen, J. Li, and S. J. Wei (2016). Seismic sensor misorientation measurement using P-wave particle motion: An application to the NECsaids array, Seismol. Res. Lett. 87, no. 4, 901–911, doi: 10.1785/0220160005
- Zhang, G., Z. Song, A. G. Osotuyi, R. Lin, and B. Chi (2022). Railway traffic monitoring with trackside fiber-optic cable by distributed acoustic sensing technology, Front. Earth Sci. 10, doi: 10.3389/feart.2022.990837
- Zheng, H., J. Fan, D. Zhao, C. Li, D. Dong, G. Zhang, and X. Wang (2020). A new method to estimate ocean-bottom-seismometer orientation using teleseismic receiver functions, Geophys. J. Int. 221, 893–904
- Zheng, H., J. Fan, D. Zhao, C. Li, D. Dong, G. Zhang, and X. Wang (2020). A new method to estimate ocean-bottom-seismometer orientation using teleseismic receiver functions, Geophys. J. Int. 221, 893–904
- Zhu, L., and H. Kanamori (2000). Moho depth variation in southern California from tele-seismic receiver functions, J. Geophys. Res. 105, no. B2, 2969–2980, doi: 10.1029/1999jb900322

INTRODUCTION
OBJECTIVES
METHODS/DATA
RESULTS
CONCLUSION

Please do not use this space, a QR code will be automatically overlayed